IOP FTC
IOP PUBLISHING SMART MATERIALS AND STRUCTURES
Smart Mater. Struct. **21** (2012) 112002 (7pp) doi:10.1088/0964-1726/21/11/112002

FAST TRACK COMMUNICATION

# Shape memory properties of ionic polymer–metal composites

**Jonathan Rossiter**[1], **Kazuto Takashima**[2] **and Toshiharu Mukai**[3]

[1] Department of Engineering Mathematics, University of Bristol, Bristol BS8 1TR, UK
[2] Graduate School of Life Science and Systems Engineering, Kyushu Institute of Technology, 2-4 Hibikino, Wakamatsu-ku, Kitakyushu 808-0196, Japan
[3] Advanced Science Institute, RIKEN, 2271-130 Anagahora, Shimoshidami, Moriyama-ku, Nagoya 463-0003, Japan

E-mail: Jonathan.Rossiter@bris.ac.uk

Received 2 July 2012, in final form 29 August 2012
Published 14 September 2012
Online at stacks.iop.org/SMS/21/112002

**Abstract**
The shape memory properties of hydrated Nafion ionic polymer–metal composite (IPMC) actuators under combined thermal cycling and electrical shape fixing are presented and experimentally demonstrated. By exploiting these new properties the utility of such ionic actuators can be greatly enhanced to include bistability, multi-modal operation and increased actuation range. Shape memory effects were shown when the IPMC was deformed during programming by either an external force or by voltage-induced actuation. Comparison is made to the shape memory effects in hydrated raw Nafion membrane. It was observed that shape memory effects undergo slow decay, with different programming methods and subsequent electrical excitation exhibiting different decay profiles.

(Some figures may appear in colour only in the online journal)

## 1. Introduction

Ionic polymer–metal composites (IPMCs) are large strain bending actuators and sensors (Tiwari and Garcia 2011, Shahinpoor and Kim 2001) which have been demonstrated in applications ranging from swimming robots (Nakabo *et al* 2007) to energy harvesters (Giacomello and Porfiri 2011). Members of the family of ionic electroactive polymers (Bar-Cohen 2004), IPMCs are triple-layer structures with a central polymer membrane sandwiched between two compliant electrodes. Electro-mechanical transduction relies on the electrically induced migration of free cations from distributed anionic binding sites to the surface cathode electrode, where Coulomb and hydraulic forces (from secondary water flux) cause local swelling and subsequent bending of the actuator. IPMCs are commonly fabricated from an ionic exchange membrane such as Nafion or Flemion, which is electroless-plated with gold or platinum (Kim and Kim 2008) and then doped with a cation such as Na+ or Li+. Alternative fabrication methods and materials have been used (see Tiwari and Garcia (2011) for a comprehensive review), and recent advances, for example through combined palladium and platinum coating (Kim and Kim 2008) and the use of ionic liquids and carbon nanotubes (Takeuchi *et al* 2009), have improved the effectiveness and versatility of ionic composite actuators. Despite these advances, IPMCs of the form described above remain those which exhibit some of the largest and fastest actuation responses.

IPMCs are bipolar devices that bend in one direction in response to a positive voltage and in the opposite direction in response to a negative voltage. Actuation is always around a central rest position, which is set by the equilibrium of mechanical forces arising from the fabrication process and from intrinsic material properties (Tiwari and Garcia 2011). A number of methods have been developed to customize the actuation of IPMCs in their post-manufacture state, including changing the cation type (Kamamichi *et al* 2007), electrically segmenting the surface electrodes (Rossiter and Mukai 2011),

 

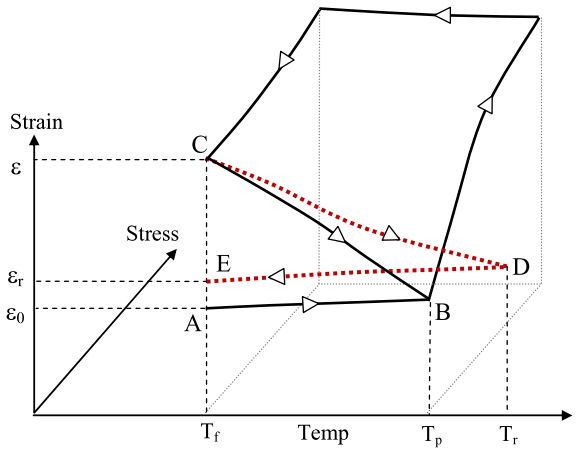


**Figure 1.** Shape memory cycle showing ideal recovery from C to B to A (solid line) and typical recovery from C to D to E (dotted line).

or by mechanically constraining the actuation, for example by using a custom mount or mechanical end-stop. These methods have limited effect on the fundamental characteristics of bipolar actuation around a central rest position. In this paper we show that Nafion-based IPMCs, in addition to their default electro-mechanical actuation, also exhibit hitherto unknown shape memory effects. These effects have the potential to overcome some of the limitations of conventional IPMCs outlined above.

Shape memory polymers have the ability to memorize a shape or deformation and to return to their original shape when appropriately stimulated, for example by light (Lendlein *et al* 2005, Koerner *et al* 2004) or heat (Liu *et al* 2007). Figure 1 shows a typical shape memory programming and recovery cycle through the stress–strain–temperature space. Shape memory materials transition from point A through B to C during shape programming. Recovery in an ideal material will involve a transition directly from C to B and then back to A. In practice, the recovery temperature $T_r$ is usually greater than the programming temperature $T_p$, and shape recovery is not always complete, i.e. the recovery ratio $R_r = (\varepsilon - \varepsilon_r)/(\varepsilon - \varepsilon_0)$ is less than unity. This is shown in figure 1 as the recovery path from C through D to E.

The demonstration of shape memory effects in ionic polymer actuators would add a new dimension to the exploitation of these smart materials and also constitutes an important consideration when operating such actuators in environments where the temperature varies. Applications that can benefit from these properties include autonomous micro-robotics and implantable medical devices (Carpi and Smela 2009). Shape memory programming also enables zero energy fixity and the consequent development of multi-stable devices (Rossiter *et al* 2006), Braille displays (Rena *et al* 2008) and minimal energy deployable structures (Conn and Rossiter 2011).

One approach to generating multi-stable and multi-functional electroactive polymers is presented in Yu *et al* (2009) and involves exploiting the shape memory properties of dielectric elastomer materials. In contrast to IPMCs, these actuators require much larger electric fields and exhibit narrow glass transition regions. Other approaches to combining actuation and shape fixity range from nanoscale shape memory effects in conducting polymers (Higgins *et al* 2011) to larger shape fixing pneumatic actuators (Takashima *et al* 2010).

In this paper we show that Nafion-based IPMCs have hitherto unknown shape memory polymer properties. We show how these may be exploited to enhance the actuation range and functionality of IPMCs. We demonstrate how shape memory programming can be achieved by external mechanical deformation and, more importantly, by the internal electro-mechanical actuation of the IPMC itself.

## 2. Shape memory effects in Nafion

Recently Xie (2010) has shown that annealed dry Nafion-117 can be programmed to 'memorize' four different shapes $(S_1, \ldots, S_4)$ within the wide glass transition temperature range ∼55–∼130 °C. This is achieved by temporarily deforming it into these shapes while cooling through the four respective fixing temperatures $T_1 \geq T_2 \geq T_3 \geq T_4$. Subsequent heating though these temperatures resulted in the recovery of the four programmed shapes in the order $S_4$, $S_3$, $S_2$, $S_1$. The attraction of Nafion over most other shape memory materials such as polyurethanes and epoxies (Liu *et al* 2007) is that, because of the very wide glass transition range due to its broad reversible phase transition, it can be programmed with a large number of unique shapes (potentially much greater than four), each of which is recovered at a different temperature. Additionally, the low voltage operation of ionic polymer actuators based on Nafion is more suitable to a number of applications such as *in vivo* devices (Wang *et al* 2005).

One interpretation of the wide glass transition range and the multi-state shape memory of Nafion is to consider the superposition of a number of narrow glass transition ranges which each only apply to a small proportion of the molecular population of the Nafion. Figure 2(a) shows a single narrow glass transition region typical of shape memory polymers and figure 2(b) shows how the wide transition curve (dashed line) of a material such as Nafion can be approximated by the set of narrow transitions $T_{g1}, \ldots, T_{gn}$ (solid lines). Figure 2(b) also shows a probability distribution (histogram in this discrete case) across the set of narrow transitions where the height represents the proportion of the material that undergoes transition at a particular temperature. This interpretation also shows how multiple states can be memorized and that memory effects at the extremes of the range will be reduced. Multi-shape programming is achieved by deforming the material into different shapes as it is cooled gradually from above $T_{gn}$ to below $T_{g1}$. Multi-shape recovery thereafter occurs as the material is heated through the series of transition temperatures from below $T_{g1}$ to above $T_{gn}$. Figure 2 shows an approximate normal distribution for illustration purposes. The precise distribution for Nafion will depend on the thermo-mechanical response as the polymer is heated, including changes in intermolecular bonding and localized phase transitions. In the reminder of this paper we will thermally cycle IPMC and hydrated Nafion in the range

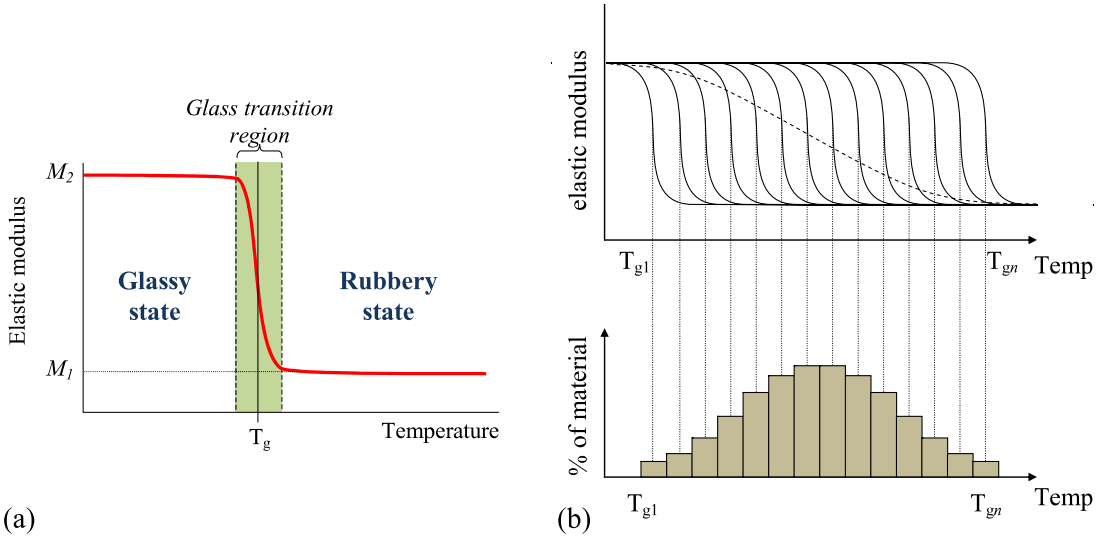


**Figure 2.** (a) Typical glass transition behaviour in a single-shape memory polymer. (b) Superposition of $n$ narrow glass transitions $\{T_{g1}, \ldots, T_{gn}\}$ (solid lines) to approximate a single wide glass transition interval $[T_{g1}, T_{gn}]$ (dashed line) capable of multi-shape memory. The lower graph shows the distribution of shape memory property at each temperature within the material.

**Table 1.** The main differences between shape memory tested Nafion and IPMCs .

| Nafion | Nafion-based IPMC |
|---|---|
| Dry | Wet |
| High temp. (140 °C annealed) | Low temp. (<80 °C) |
| Compressed (dehydrated) | Swollen (hydrated) |
| Reduced moieties (Xie and Hayden 2007) | Significant ionic content |
| Nafion membrane only | Metal electrodes |
| Thermal processes | Chemical processes |

(28 °C, 80 °C), within the lower half of the shape memory range of Nafion.

Although raw Nafion has been shown to have attractive shape memory Properties, there are significant differences between the Nafion tested by Xie (2010) and the IPMCs tested here. Table 1 summarizes the main differences.

Of the differences outlined in table 1 these can be divided into mechanical constraints (metal electrodes) intermolecular differences (swelling), thermal differences and ionic/chemical differences. Conservatively, we might expect at least one, if not all, of these to alter or even eliminate the shape memory behaviour in Nafion IPMCs. We will now investigate shape memory effects in IPMCs using both mechanical and electrically induced deformations during the shape fixing (programming) process.

## 3. Thermo-mechanical fixing of shape memory IPMCs

In order for shape memory effects in Nafion IPMCs to be verified, they must show actuation that is different in some way when in a programmed state in comparison to their default as-fabricated state. For example the IPMC may undergo a change in rest position, or it could exhibit a different actuation modality, such as rotation or linear actuation.

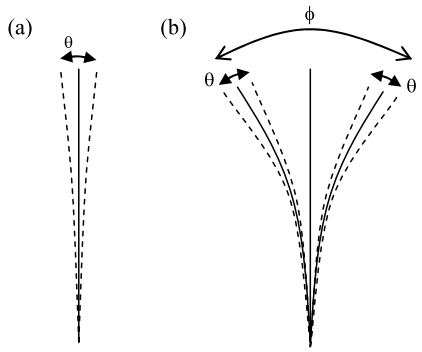


**Figure 3.** Shape memory programming of an IPMC can result in change in rest position and consequent increase in net actuation range from $\theta$ to $\phi$: (a) as-manufactured IPMC; (b) change in reset position to left or right.

Figure 3 shows how changing the rest position of the actuator can increase the net actuation range of an IPMC from $\theta$ to $\phi$.

To evaluate thermal–mechanical shape memory programming in order to change IPMC actuation modality, a 30 mm × 4 mm sample of 127 $\mu$m thick, Nafion-115 IPMC was fabricated using three cycles of the Ogura/Asaka electroless gold plating method (Fujiwara *et al* 2000) and doped with Na+ cations, as shown in figure 4(a). The sample was then wrapped around a glass rod and held in place while it was immersed in a water bath at the programming temperature $T_p = 60$ °C for 3 min then cooled in a water bath at the fixing temperature of $T_f = 28$ °C. Upon removal from the glass rod the spiral shape in figure 4(b) had been fixed. This structure is similar to that fabricated in Li *et al* (2011) and shows a 900° (5$\pi$ rad) spiral. In contrast to the original flat shape (figure 4(a)) that bends when electrically stimulated, this structure exhibits rotational actuation. To show shape recovery the spiral actuator was then immersed in a water bath at the recovery temperature of $T_r = 80$ °C for 5 min then cooled in

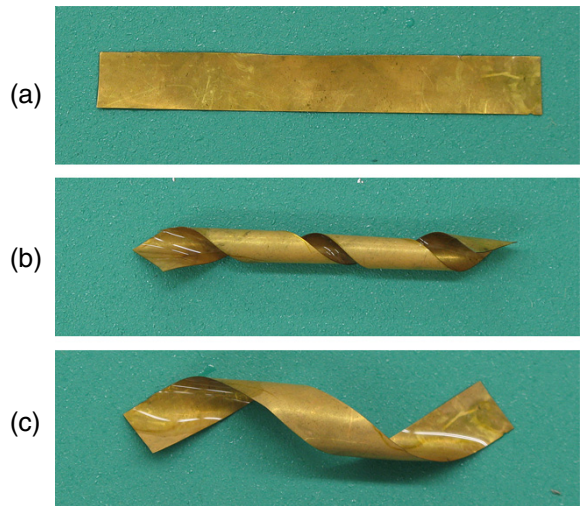


**Figure 4.** IPMC undergoing thermo-mechanically induced shape memory cycle: (a) original shape; (b) programmed shape; (c) recovered shape.

a water bath at $T_f = 28\,°C$. The recovered shape shown in figure 4(c) has a residual spiral of 360°, representing a 60% shape recovery in terms of rotational deformation. This shows that thermo-mechanical shape memory effects are present in Nafion IPMCs. Clearly recovery is not complete and this may be due not only to the differences outlined in table 1 but also to the relatively tight spiral of the programmed shape and the relatively thin Nafion-115 IPMC. In this experiment Nafion-115 was employed instead of the thicker Nafion-117 used in subsequent experiments. The thinner Nafion-115 was found to be more easily wrapped into the tight spiral in figure 4. We expect the fundamental shape memory behaviour of the Nafion membrane within the two thicknesses to be the same. Note that the Nafion-115 is three-times gold plated, in contrast to the five-times plating of the Nafion-117, resulting in thinner electrodes. The thicknesses of the electrodes as a percentage of the overall thickness of both types of IPMC are approximately equal at about 10%.

## 4. Thermo-electrical fixing of shape memory IPMCs

While mechanical shape fixing and recovery of IPMCs has been shown above, the attraction of IPMCs over other shape memory polymers is that, instead of mechanically deforming the polymer during shape programming, the deformation can be electrically induced by exploiting the electro-mechanical coupling of the polymer actuator. The process of electrically fixing an IPMC therefore involves five steps.

(1) The IPMC is initially unactuated and at its rest position.
(2) It is then heated to the programming temperature $T_p$.
(3) DC voltage $V_f$ is applied and the IPMC bends.
(4) The IPMC is cooled to the fixing temperature $T_f$.
(5) DC voltage is removed.

To evaluate the thermo-electrical shape memory property a series of experiments was undertaken. Five-times electroless

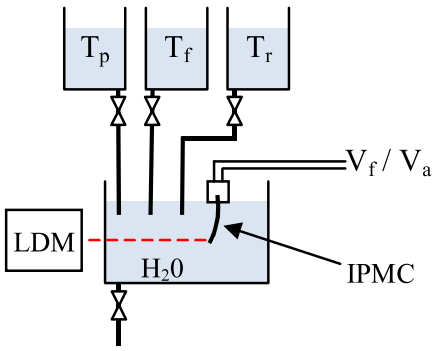


**Figure 5.** Experimental setup for thermo-electric shape memory programming of IPMCs.

coated 175 $\mu$m thick Nafion-117 IPMCs were cut into 30 mm × 4 mm samples. These samples were doped with TEA+ ions by soaking them in 0.1 M ionic solution for 24 h. The TEA+ ion is relatively large and generates a slower response than smaller Na+ or H+ cations but with markedly less back-relaxation (Yamakita *et al* 2006). Slow back-relaxation is important in our tests because the rate of change of temperature of the IPMC is limited by the use of water to perform heating and cooling of the hydrated samples. Figure 5 shows the experimental setup where the IPMC cantilever is mounted vertically in a tank and where the tank can be filled with water at the programming, fixing and recovery temperatures $T_p$, $T_f$ and $T_r$ respectively. AC actuation signal $V_a$ and DC fixing voltage $V_f$ can be applied through the mounting clip. A Keyence laser displacement meter measures displacement of the IPMC 12 mm below the tip. Actuation tests are performed before fixing, after fixing and after recovery, and involve applying a square wave of amplitude $V_a$ volts and frequency 0.5 Hz. Recovery involves heating to the recovery temperature $T_r$ with no electrical stimulation.

The measured displacement profile for an IPMC undergoing thermo-electrical shape memory programming is shown in figure 6. This shows two shape memory cycles: negative voltage-induced fixing and recovery, followed by positive voltage-induced fixing and recovery. During shape programming the actuator was fixed when at its maximum voltage-induced displacement, with negligible back-relaxation. Figure 6 shows the mean actuation response at the start (i), after first shape memory programming (ii), after shape recovery (iii), after second, reverse fixing (iv), and after final recovery (v). Figure 7 shows the actuation responses for states (i)–(v) in figure 6. Note that the rest position is shifted over a range of approximately 2.7 mm while the amplitude of the actuation response remains approximately 0.2 mm. The actuation and fixing voltages ($V_a = 0.5$ V, $V_f = 1$ V) were chosen to fit the measurement constraints of the experiment. During preliminary experiments larger actuation voltages up to $V_a = V_f$ were tested and shape memory effects were observed to be consistent with the results presented here.

After negative voltage programming (state (ii)) the initial actuation rest position has moved to −1.5 mm. After recovery (state (iii)) the rest position recovers, with some residual shape

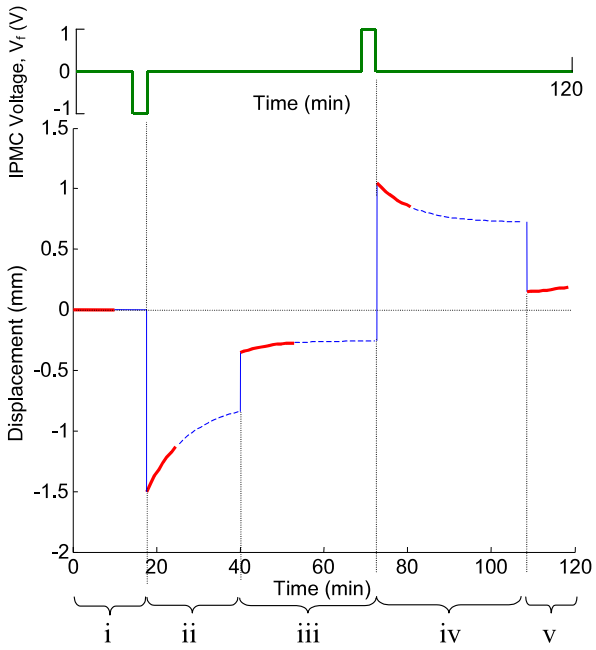


**Figure 6.** Shape memory programming and recovery in IPMCs ($V_f = \pm 1$ V) (red lines show experimental data and dashed lines show exponential extrapolations).

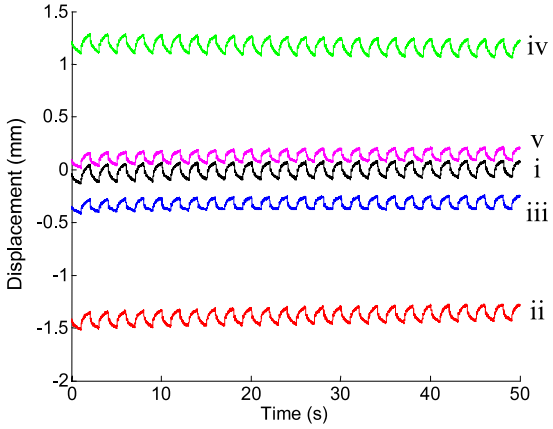


**Figure 7.** Actuation responses for states (i)–(v) in figure 6 ($V_a = 0.5$ V, 0.5 Hz).

fixing remaining (approximately 27%). By applying a small reverse electrical bias during recovery we can expect full recovery. The graph shows clear shape programming in state (ii) and state (iv), and shape recovery in states (iii) and (v). Figure 6 also shows an element of long term decay in the programmed states. This decay is consistent with the results in Xie (2010) for dry annealed Nafion.

## 5. Decay effects in shape memory IPMCs

To determine the rate and limits of decay in the programmed shape, further experiments were undertaken. In these cases no recovery was performed after shape programming. Instead, the deflection of the tip of the shape-programmed IPMC was monitored for approximately 45 min, during which time

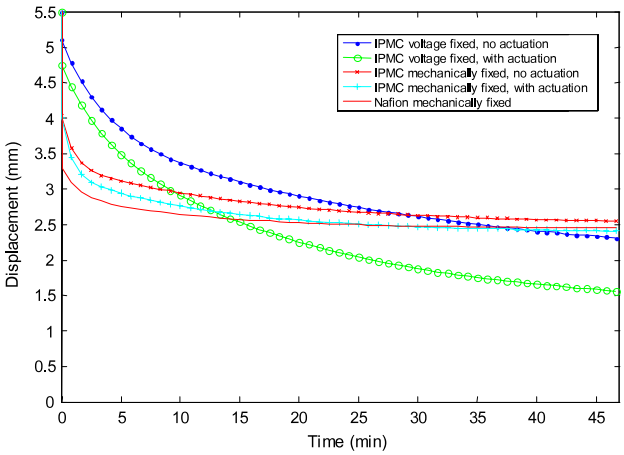


**Figure 8.** Decay of programmed deformation in IPMCs and raw Nafion. All samples programmed with displacement 5.5 mm at time $t = 0$.

the IPMC was either actuated intermittently as before ($V_a = 0.5$ V, 0.5 Hz for 100 s then 90 s rest), or left to decay without actuation.

To compare the decay of shape memory effects in IPMCs to those of raw Nafion, samples of Nafion-117 the same size as the IPMCs (30 mm × 4 mm) were cut from a large membrane. This was the same Nafion membrane from which the IPMC had been fabricated. Note that the Nafion samples had not been thermally annealed or otherwise processed, but had been fully hydrated in deionized water. These Nafion samples underwent the same experimental procedure as described above, but no actuation tests were performed and the samples were programmed by mechanically deflecting the tip. Figure 8 shows shape memory decay (in terms of tip displacement) for the four IPMC and one Nafion cases after shape fixing. In all instances the tip of the sample was displaced by 5.5 mm during shape fixing, either by voltage ($V_f = 2$ V) or mechanical means (a metal block as described in Rossiter *et al* (2012)). Note that for large deflections the bending stresses imposed by the two different fixing methods result in different profiles. That is, voltage fixing results in a near uniform curvature while mechanical fixing introduces more bending at the base, in line with Euler beam theory. At the small deflections employed in these experiments minor differences in profiles were observed and were assumed small enough to have negligible effects. Future work will consider the induced stress distributions, and their effects on shape memory programming, in more detail.

It is clear from figure 8 that all samples undergo a degree of decay in their programmed displacement. After 45 min samples show up to 50% remaining programmed displacement. There is also a marked difference between the samples fixed by mechanical means in comparison to those fixed by voltage. The voltage fixed samples show a slower initial decay but have a lower final displacement. Mechanically fixed samples, on the other hand, show faster initial decay but have a larger final displacement. Also evident is the faster decay and lower final displacement of samples undergoing intermittent actuation tests throughout the 45 min.

It was further observed that decay within the actuation periods occurs at a slightly greater rate than in neighbouring periods of no actuation. These indicate that, although the electrical excitation of the fixed composite does slightly affect shape memory stability, i.e. the two effects are loosely coupled, the choice of fixing mechanism has a larger effect on the shape of the decay graph. It is interesting to also note that mechanically fixed raw Nafion shows a decay profile similar to the mechanically fixed IPMCs. Given the decay profiles evident in figure 8, the conventional static shape fixity ratio $R_f$ (Xie 2010) cannot be said to capture the time-dependent nature of decay. Instead, tip displacement can be effectively described as the second order exponential function $d(t) = d_0 + \beta e^{(-t/\gamma)} + \chi e^{(-t/\varphi)}$, where convergence values are $d_0 = \{1.34, 1.95, 2.50, 2.39, 2.43\}$ mm for the five cases in figure 6. (For brevity, coefficients $\beta$, $\gamma$, $\chi$ and $\varphi$ are not given.) All samples, save one, converge on final displacements with fixity ratios exceeding 35%.

## 6. Fixing mechanisms

Since the mechanically fixed Nafion and IPMC samples exhibit similar decay profiles we can posit that the IPMC fabrication process and the presence of metal electrodes does not markedly change the fundamental shape memory properties of the polymer at these low strains. On the other hand, the difference between voltage-induced and mechanical-induced fixing in figure 8 suggests that electrically induced effects inside the IPMC do affect shape decay. Likely causes include the disruption of functional moieties in the Nafion (possibly exaggerated by thermal effects (Xie and Hayden 2007)) and local density changes as cations migrate to the cathode and pull water molecules with them. These density changes may alter the temperature-dependent bonds that the shape memory effect in Nafion relies upon. This is in agreement with Park *et al* (2007), which noted that hydration resulted in disconnected polymer chains, volumetric changes and plasticization. It is interesting to note that the material strains here are small (<2%), which results in a relatively small change in molecular orientation and compression (van der Heijden *et al* 2004). Much larger strains are reported in Xie (2010) and these may exaggerate the shape memory effects in Nafion.

## 7. Conclusions

We have demonstrated that ionic polymer–metal composites fabricated from Nafion ion-exchange membrane have significant shape memory effects. This has two important consequences: (1) shape memory effects can be used to enhance the range and sophistication of IPMC actuators, and (2) these shape memory effects will change the actuation response with temperature and these must therefore be taken into account when IPMCs are used in applications where the temperature changes. We have shown that IPMCs have an important facility enabling exploitation of shape memory effects: namely, the ability to deform into a fixing shape by electrical stimulation. Thus no external mechanical stimulation is needed during the shape programming or recovery processes. Both the thermo-mechanically and thermo-electrically fixed shapes show slow decay towards the as-fabricated shape, consistent with the decay shown for raw Nafion and resulting in long-term shape fixing of more than 35% deformation with respect to the initial programmed shape.

The shape memory effects demonstrated here are extremely attractive for new applications of ionic actuators, from micro-MEMS devices to larger artificial muscles. Future work will investigate the relationship between chemical and mechanical structures and actuation mechanisms of Nafion-based ionic polymers and the shape memory properties presented here.

## Acknowledgment

This work was funded by the UK Engineering and Physical Sciences Research Council under grant EP/F022824/1.

## References

Bar-Cohen Y (ed) 2004 *Electroactive Polymer (EPA) Actuators as Artificial Muscles: Reality, Potential, and Challenge* 2nd edn (Bellingham, WA: SPIE Optical Engineering Press)

Carpi F and Smela E (ed) 2009 *Biomedical Applications of Electroactive Polymer Actuators* (New York: Wiley)

Conn A T and Rossiter J 2011 Smart radially folding structures *Smart Mater. Struct.* **21** 035012

Fujiwara N, Asaka K, Nishimura Y, Oguro K and Torikai E 2000 Preparation of gold-solid polymer electrolyte composites as electric stimuli-responsive materials *Chem. Mater.* **12** 1750–4

Giacomello A and Porfiri M 2011 Underwater energy harvesting from a heavy flag hosting ionic polymer metal composites *J. Appl. Phys.* **109** 084903

Higgins M J, Grosse G, Wagner K, Molino P J and Wallace G G 2011 Reversible shape memory of nanoscale deformations in inherently conducting polymers without reprogramming *J. Phys. Chem.* B **115** 3371–8

Kamamichi N, Yamakita M, Kozuki T, Asaka K and Luo Z W 2007 Doping effects on robotic systems with ionic polymer–metal composite actuators *Adv. Robot.* **21** 65–85

Kim S-M and Kim K J 2008 Palladium buffer-layered high performance ionic polymer–metal composites *Smart Mater. Struct.* **17** 035011

Koerner H, Price G, Pearce N A, Alexander M and Vaia R A 2004 Remotely actuated polymer nanocomposites—stress-recovery of carbon-nanotube-filled thermoplastic elastomers *Nature Mater.* **3** 115–20

Lendlein A, Jiang H, Junger O and Langer R 2005 Light-induced shape-memory polymers *Nature* **434** 879–82

Li S-L, Kim W-Y, Cheng T-H and Oh I-K 2011 A helical ionic polymer–metal composite actuator for radius control of biomedical active stents *Smart Mater. Struct.* **20** 035008

Liu C, Qin H and Mather P T 2007 Review of progress in shape-memory polymers *J. Mater. Chem.* **17** 1543–58

Nakabo Y, Mukai T and Asaka K 2007 Biomimetic soft robots using IPMC *Electroactive Polymers for Robotic Applications: Artificial Muscles and Sensors* ed K J Kim and S Tadokoro (London: Springer)

Park I-S, Kim S-M and Kim K J 2007 Mechanical and thermal behavior of ionic polymer–metal composites: effects of electroded metals *Smart Mater. Struct.* **16** 1090

Ren K, Liu S, Lin M, Wang Y and Zhang Q M 2008 A compact electroactive polymer actuator suitable for refreshable Braille display *Sensors Actuators* A **143** 335–42

Rossiter J, Stoimenov B and Mukai T 2006 A self-switching bistable artificial muscle actuator *Proc. SICE-ICASE* 5847–52

Rossiter J M and Mukai T 2011 Electrostatic and thermal segmentation of multi-segment IPMC sensor-actuators *Proc. SPIE* **7976** 1–8

Rossiter J M, Takashima K and Mukai T 2012 Enhanced IPMC actuation by thermal cycling *Proc. SPIE* **8340** 1–7

Shahinpoor M and Kim K J 2001 Ionic polymer–metal composites: I. Fundamentals *Smart Mater. Struct.* **10** 819

Takashima K, Rossiter J and Mukai T 2010 McKibben artificial muscle using shape-memory polymer *Sensors Actuators* A **164** 116–24

Takeuchi I, Asaka K, Kiyohara K, Sugino T, Terasawa N, Mukai K, Fukushima T and Aida T 2009 Electromechanical behavior of fully plastic actuators based on bucky gel containing various internal ionic liquids *Electrochim. Acta* **54** 1762–8

Tiwari R and Garcia E 2011 The state of understanding of ionic polymer metal composite architecture: a review *Smart Mater. Struct.* **20** 083001

van der Heijden P C, Rubatat L and Diat O 2004 Orientation of drawn nafion at molecular and mesoscopic scales *Macromolecules* **37** 5327–36

Wang Y, Bachman M, Li G-P, Guo S, Wong B J F and Chen Z 2005 Low-voltage polymer-based scanning cantilever for *in vivo* optical coherence tomography *Opt. Lett.* **30** 53–5

Xie T 2010 Tunable polymer multi-shape memory effect *Nature* **464** 267–70

Xie T and Hayden C A 2007 A kinetic model for the chemical degradation of perfluorinated sulfonic acid ionomers: weak end groups versus side chain cleavage *Polymer* **48** 5497–506

Yamakita M, Sera A, Kamamichi N, Asaka K and Luo Z-W 2006 Integrated design of IPMC actuator/sensor *Proc. ICRA* 1834–9

Yu Z, Yuan W, Brochu P, Chen B, Liu Z and Pei Q 2009 Large-strain, rigid-to-rigid deformation of bistable electroactive polymers *Appl. Phys. Lett.* **95** 192904